THE JOURNAL OF PHYSICAL CHEMISTRY B

Article

pubs.acs.org/JPCB

# Simulating the Interaction between Amino Acids and DNA: A Combined Matrix-Isolation FT-IR and Theoretical Study of the 1-Methyluracil·Glycine H-Bond Complexes Using a Dual Sublimation Furnace

Bram Boeckx* and Guido Maes

Department of Chemistry, University of Leuven, Celestijnenlaan 200F, Leuven, Belgium

Supporting Information

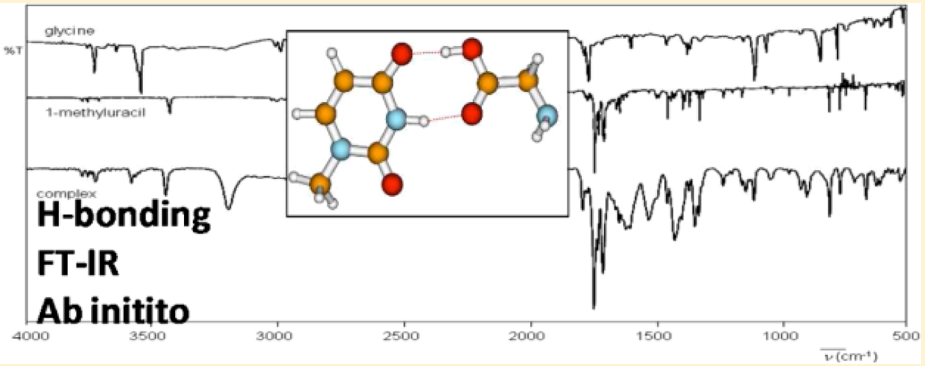


**ABSTRACT:** The H-bond complex formation between 1-methyluracil and glycine has been investigated by theoretical calculations and the most stable complex configurations have been identified by FT-IR spectroscopy in Ar matrices. The importance of this H-bonding system is huge since all DNA biological functions are dependent on the interactions with proteins. The theoretical optimizations have revealed six different closed H-bond complexes between 1-methyluracil and glycine. The obtained energies have demonstrated that the uracil $C^4{=}O$ site is a better H-acceptor site than the $C^2{=}O$ site. The stabilization energy of the most stable complex is −47.83 (MP2) or −54.14 kJ·mol$^{-1}$ (DFT). The DFT(B3LYP)/6-31G optimized geometries have been evaluated, and the obtained energies appeared to be in agreement with the results of the computational more expensive DFT(B3LYP)6-31++G** approach. In order to identify the 1:1 complexes in an argon matrix, a new dual miniature furnace has been developed which allows to sublimate both complex partners at their optimal temperature. The presence of three different glycine·1-methyluracil complexes has been demonstrated by analysis of the H-bond shifted modes. The H-bond parameters have been evaluated and previously obtained correlations for different H-bond complexes have been confirmed.

## INTRODUCTION

DNA plays a key role in the development and functioning of living organisms for the storage and transfer of the genetic information. All DNA functions are dependent on the interactions with proteins.[1−6] H-bonds are important in view of the interactions between proteins and nucleic acids, since they have a crucial contribution to the structural stability of DNA and proteins. Therefore, forming or breaking H-bonds is involved in nearly all the protein nucleic acid interactions. Moreover, many of these interactions are directly dominated by H-bonds.[7,8] Multiple H-bonds have been proposed to be the crucial directing element in the molecular recognition process in protein nucleic acid complexes.[9−13] It has been investigated that the H-bond interaction between nucleic acids and proteins is an essential factor in the glycosidic bond cleavage[1] and in the repair of oxidative damage of purines.[9−11] The H-bond interaction between the amino acid side chain and DNA bases influences the electronic properties of the nucleic acid base[14] which plays an important role in the understanding of DNA and RNA damaging.[15−17]

In view of the huge importance of H-bonding between proteins and DNA, we have investigated the H-bonded complex between two of the most elementary building blocks of these biopolymers, i.e., the simplest amino acid glycine and the modified RNA base 1-methyluracil. 1-Methyluracil can be considered as a suitable model for uridine which occurs in RNA, since the heavy methyl group at the N1 position simulates reasonably well the ribose moiety in terms of the vibrational properties of uracil. Although this system is definitely simpler than real biochemical targets, and, important

**Received:** July 15, 2012
**Revised:** August 31, 2012
**Published:** September 10, 2012

   dx.doi.org/10.1021/jp307388e | J. Phys. Chem. B 2012, 116, 11890−11898

to note, this study is performed in a simulated ideal gas phase where no zwitterions occur which includes no real biological environment, these interactions can provide a first insight into real biochemical problems.[18]

Matrix isolation is an extremely suitable technique to study these interactions[19] on the molecular level. The formation of an intermolecular complex X—H···B is governed by the equilibrium condition $\Delta G^\circ = -RT \ln K = \Delta H^\circ - T\Delta S^\circ$. Because in matrix-isolation conditions complex formation occurs very close to the extremely cold CsI window, the term $T\Delta S^\circ$ can be neglected, which implies that, in these extreme conditions, the equilibrium is strongly shifted toward the complex compared to the equilibrium at room temperature.

A challenging and important issue for the experimental formation and identification of 1:1 complexes of two complex partners such as glycine and 1-methyluracil is how to sublimate both complex partners at their own sublimation temperature. Sublimation of both compounds from a solid mixture in the same furnace would give rise to di-, tri-, or multimers of the compound with the lowest sublimation temperature which must be avoided. For this reason, a new dual mini furnace was developed. In this way, both complex partners could be sublimated out of the furnace at their own sublimation temperature. This innovative dual furnace can be used to study an extended range of new complexes which is important since molecular complexes are precursors for bimolecular reactions.[20]

Early theoretical HF (Hartree−Fock) investigations of H-bond interactions of amino acids and nucleic acids on the molecular level have revealed that the stabilizing or destabilizing effect of the intermolecular H-bonds on the base pairs mainly depends on the site and the type of the interaction.[21,22] The interaction between polyglycine and $\beta$-DNA helices has been studied using the HF level.[23] The free energies of the interactions of the asparagine side chain and nucleobase pairs have been studied by the molecular force field methodology.[24] Post-Hartree−Fock theoretical studies have been performed on interactions between glycine and the most[25,26] or minor[27] abundant uracil tautomers. The most stable complexes found in these studies appeared to be those with the carboxylic group of glycine bonded by through two H-bonds to uracil in a closed H-bonded complex. The interaction energy of these complexes was found to be about −50 to −60 kJ·mol$^{-1}$. A computational study of the H-bond complexes between the most stable leucine rotamers and RNA bases at the DFT level of theory has also revealed that the most stable complexes were closed H-bond configurations, the largest with stabilization energies up to −71 kJ·mol$^{-1}$.[18] Recently, the H-bond interaction between glycine and 5-fluorouracil has been theoretically investigated.[28] Heteroassociation by H-bonding of the uracil derivatives 5-fluorouracil, 5-chlorouracil, and 5-methyluracil (thymine) with cysteine have been studied at the DFT(B3LYP)/6-311++G** level of theory.[29] The binding energies of heterodimerization were found to be −52 to −66 kJ·mol$^{-1}$.

In contrast to this wide range of theoretical studies on H-bonded complexes of nucleic acids and their derivatives (e.g., refs 30−33), there are few experimental studies revealing the intrinsic molecular properties of nucleic acid·amino acid complexes. The role of the amide group in untwisting the double helix has been investigated.[34−36] Complexes of 1-methyluracil and methylated cytosines with acrylamide have been studied by mass spectroscopy in combination with theoretical calculations.[34,37] These studies have revealed closed H-bonded complexes with theoretical interaction energies of about −60 kJ·mol$^{-1}$. Photoelectron spectroscopy experiments have been performed in combination with supporting theory on the anionic form of the uracil·glycine[38] and thymine·glycine[39] complexes. Recently, the photoelectron spectrum for three-body complexes between 1-methylthymine, 9-methyladenine, and formic acid anions has been recorded and interpreted through quantum-chemical modeling carried out at the B3LYP/6-31+G(d,p) level, which also revealed closed H-bonded complexes.[40]

In this paper, we present the results of a matrix-isolation Fourier transform infrared (FT-IR) investigation, using a newly developed dual furnace combined with a theoretical investigation of the possible H-bonded complex between 1-methylyracil and glycine. The matrix-isolation FT-IR spectra of the monomers have previously been reported by our the research group.[41−44]

## THEORETICAL METHODOLOGY

The geometries of the most stable complexes between 1MU and glycine have been investigated by Hartree−Fock (HF) and density functional theory, including Becke's nonlocal hybrid three-parameter exchange functional[44] in combination with the Lee−Yang−Parr correlation functional DFT(B3LYP)[45,46] optimizations. Moller−Plesset second-order perturbation theory (MP2)[47] single-point energy calculations starting from the DFT-optimized geometries of the monomers have also been performed. A valence-split double-$\zeta$ basis set, 6-31G was used which was expanded in some cases with diffuse and polarization functions.

Frequency calculations were performed to the obtained minima, and the IR frequencies were corrected for the effect of anharmonicity using variable scaling factors suitable for small biomolecules,[48−50] i.e., 0.95 for $\nu$(X−H), 0.98 for $\gamma$ and $\tau$, 0.975 for all other modes, and 0.97 for the zero-point energy (ZPE).

The computational calculations were performed using the Gaussian 03 software package[51] available on the high-performance computing Linux cluster of the University of Leuven. A special software package designed by Dr. L. Lapinski (Institute of Physics, Polish Academy of Sciences, Warsaw, Poland) was used to calculate the potential energy distributions (PED) of each frequency.[52] This theoretical approach has been successfully applied in the past for the comparison with matrix-isolation spectra of similar monomeric compounds.[48,53−56]

## EXPERIMENTAL METHODOLOGY

The FT-IR spectra have been recorded with a Bruker IFS66 spectrophotometer at a resolution of 1 cm$^{-1}$. To create a matrix with a sufficient amount of 1:1 complexes, a new dual furnace was developed and optimized (Figure 1). In this way, both monomers could be sublimated at their specific sublimation temperatures. The apertures of the furnaces were closely to each other and directed toward a cryogenic CsI window which was cooled to 16 K. The optimal sublimation temperature of glycine was found to be 343 and 313 K for 1MU in this setup combined with a $1.0 \times 10^{-5}$ mbar Ar pressure in the cryostat. These conditions resulted after 4 h of deposition, in a sufficient yield of the 1:1 heterocomplex, and prevented decomposition of the compounds by formation of homomultimers.

1MU and glycine were purchased from Aldrich (>99%) and high-purity argon gas (99.99990%) from Air Liquid was used.

**Figure 1.** Dual miniature furnace constructed for this work.

## RESULTS

In the search for the most stable glycine·1-methyluracil complexes, the theoretical optimizations were started from the optimized geometries of the separate monomers.

For 1-methyluracil the study is limited to the keto tautomer (Figure 2). Since the energy difference with the enol tautomers

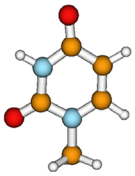

**Figure 2.** The most stable tautomer of 1-methyluracil.

is very large ($E_{DFT}$ > 40 kJ·mol$^{-1}$), the keto form is the only tautomer observable in the low-temperature matrix. This is also reasonable since tautomers have rarely been observed in oligonucleotide crystals, e.g., for 1MU,[57] and for most biological processes only one major tautomer of this base is involved.[18]

It has been demonstrated in previous research that the complex partner glycine occurs in three different conformations in an argon matrix.[41,58] The previously obtained geometries are presented in Figure 3, and the associated energies differences

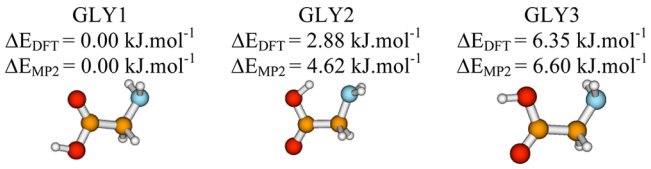


**Figure 3.** Optimal geometries and relative energies (DFT(B3LYP)/6-31++G** and MP2/6-31++G**) of the most stable conformations of glycine.

obtained with the method used in this study are summarized in Table 1. The important theoretical and observed FT-IR frequencies of glycine and 1-methyluracil in the argon matrix and extended energy data are included in the Supporting Information.

In the three conformations of glycine, three possible H-bond donor sites are available, i.e., $NH_2$ and OH while N and C═O are possible acceptor sites. On the other hand, the only stable tautomer of 1-methyluracil has one H-bond donor site ($N^3$–H) and two acceptor sites ($C^4$═O and $C^2$═O). As a matter of fact, two possible closed H-bond complexes between GLY and 1MU are theoretically possible for each of the three glycine conformations, i.e., one with $C^2$═O as the acceptor site and one with $C^4$═O as the acceptor site, both with the $N^3$H of

**Table 1. DFT(B3LYP)/6-31++G** and MP2/6-31++G** Energies (au), Zero-Point Vibrational Energies (ZPE, au), Relative Energies (Δ*E*, au), and Dipole Moments (*μ*, D) for the Most Stable Conformations of Glycine**

| conformation | $\Delta E^a$ | $\Delta E^b$ |
|---|---|---|
| GLY1 | 0.00 | 0.00 |
| GLY2 | 2.88 | 2.82 |
| GLY3 | 6.35 | 6.30 |
| GLY1 | 0.00 | 0.00 |
| GLY2 | 4.62 | 3.96 |
| GLY3 | 6.60 | 7.14 |

[a]Energy difference between the different conformations relative to the most stable conformation GLY1. [b]DFT data obtained by Ramaekers et al.[58] at the DFT(B3LYP)/6-31++G** level of theory; MP2 data obtained by Stepanian et al.[57] at the MP2/aug-cc-pVDZ level of theory.

1MU as H-bond donor. These six configurations were optimized at the consecutive HF/3-21G, DFT(B3LYP)/3-21G, DFT(B3LYP)/6-31G, and DFT(B3LYP)/6-31++G** levels of theory. The obtained electronic energies at the various theoretical levels are listed in Table 2, and the different complex configurations are presented in Figure 4 which also contains the ZPE-corrected energies.

**Table 2. Relative Electronic HF and DFT(B3LYP) Energies[a] (kJ·mol$^{-1}$) with Different Basis Sets for Different Configurations of the Complex Glycine·1-Methyluracil**

| | relative energies[a] | | | | | |
|---|---|---|---|---|---|---|
| level of theory | **1** | **2** | **3** | **4** | **5** | **6** |
| HF/3-21G | 0.00 | 3.95 | 5.61 | 10.00 | 46.10 | 47.83 |
| DFT(B3LYP)/3-21G | 0.00 | 8.89 | 3.34 | 12.92 | 30.22 | 37.08 |
| DFT(B3LYP)/6-31G | 0.00 | 6.23 | 4.29 | 11.16 | 29.65 | 33.88 |
| DFT(B3LYP)/6-31++G** | 0.00 | 4.83 | 4.42 | 9.80 | 26.44 | 30.00 |

[a]Relative to complex **1**. Absolute values for complex **1**: *E*(HF/6-31G) = −730.264 886 au, *E*(DFT(B3LYP)/3-21G) = −734.517 309 au, *E*(DFT(B3LYP)/6-31G) = −738.346 925 au, *E*(DFT(B3LYP)/6-31++G**) = −738.638 658 au.

Since the CPU time of complexes with amino acids larger than glycine are expected to be extremely long, single-point energy calculations at the DFT(B3LYP)/6-31++G** and MP2/6-31++G** levels of theory were performed on the

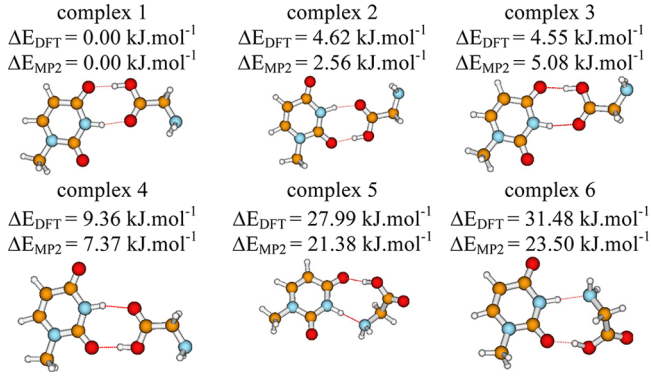


**Figure 4.** Optimal geometries and relative energies (DFT(B3LYP)/6-31++G** and MP2/6-31++G**) of the most stable configurations of the complex glycine·1-methyluracil.


dx.doi.org/10.1021/jp307388e | J. Phys. Chem. B 2012, 116, 11890–11898

obtained DFT(B3LYP)/6-31G geometries. In this way, the accuracy of these geometry calculations can be tested and unnecessary long CPU time requiring optimizations can be possibly avoided for larger systems. The relative energy differences resulting from these single-point calculations are compared to those obtained after DFT(B3LYP)/6-31++G** optimization in Table 3.

**Table 3. Comparison between the Single Point (SP) DFT(B3LYP)/6-31++G** and MP2/6-31++G** Relative Electronic Energies (kJ·mol$^{-1}$) on DFT(B3LYP)/6-31G and DFT(B3LYP)/6-31++G** Optimized Geometries**

| | relative energies[a] | | | | | |
|---|---|---|---|---|---|---|
| level of theory | 1 | 2 | 3 | 4 | 5 | 6 |
| Optimized at DFT(B3LYP)/6-31G | | | | | | |
| SP[a] DFT(B3LYP)/6-31++G** | **0.00** | **4.56** | **3.97** | **9.10** | **27.18** | **18.35** |
| Opt. DFT(B3LYP)/6-31++G** | **0.00** | **4.83** | **4.42** | **9.80** | **26.44** | **30.00** |
| SP[a] MP2/6-31++G** | 0.00 | 1.09 | 4.37 | 5.83 | 19.15 | 19.81 |
| Optimized at DFT(B3LYP)/6-31++G** | | | | | | |
| DFT(B3LYP)/6-31G | 0.00 | 6.23 | 4.29 | 11.16 | 29.65 | 33.88 |
| DFT(B3LYP)/6-31++G** | 0.00 | 4.83 | 4.42 | 9.80 | 26.44 | 30.00 |

[a]DFT(B3LYP)/6-31G optimized geometries. [b]DFT(B3LYP)/6-31++G** optimized geometries.

From this table it is clear that the relative electronic energy differences for the low-energy configurations (complexes **1**−**5**) obtained after optimization at the DFT(B3LYP)/6-31++G** level of theory do not significantly differ from the ones obtained by the single-point energy calculations at DFT(B3LYP)/6-31G configurations. The results of the MP2 single-point calculations on the configurations of both levels give less satisfying results. These results demonstrate that optimizations at the DFT-(B3LYP)/6-31G level in compination with singe-point DFT-(B3LYP)/6-31++G** are acceptable for our purpose, i.e., a prediction of the stability of the different complex configurations. This conclusion is important to save CPU time for larger systems with similar molecules.

Frequency analysis has been performed on the DFT-(B3LYP)/6-31++G** level of theory on the configurations obtained at that level. The results for the energies are presented in Figure 4 and the extended results can be found in the Supporting Information.

As far as the most stable configurations (Figure 5) are concerned, we observe that the configurations of complex **1** and complex **2** are both formed with the most stable glycine conformation, GLY1, characterized by a bifurcated $NH_2\cdots O{=}C$ H-bond. In both these configurations, the OH and the C=O group of the amino acid are the H-bond donor and acceptor, respectively, which form H-bonds with the C=O and the NH groups of the base. In complex **1**, the $C^4{=}O$ group and in complex **2** the $C^2{=}O$ group of 1MU is involved in the intermolecular H-bond. The bifurcated intramolecular H-bond $NH_2\cdots O{=}C$ of GLY1 still exists in both complexes. Complexes **3** and **4** are formed with the conformation GLY3, containing a weak $NH_2\cdots O(H)$ H-bond. Similar to the complexes **1** and **2**, the OH and the C=O groups are the respective H-bond donor and acceptor in the amino acid whereas the NH and the C=O are the H-bond sites of 1MU. In complex **3**, the $C^4{=}O$ and in

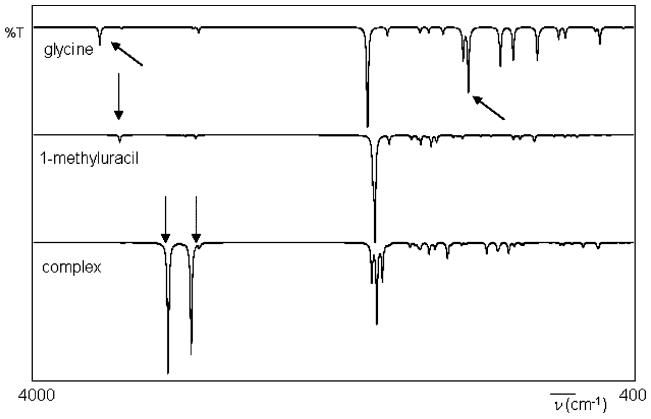


**Figure 5.** Theoretical (DFT) transmission (% T) IR spectra of the most abundant conformation of glycine, the keto tautomer of 1-methyluracil and the most stable complex glycine·1-methyluracil. The important shifted modes due to the complex formation are indicated by arrows.

the less stable complex **4** the $C^2{=}O$ group is involved in the intermolecular H-bond. Complexes **5** and **6** are complexes withGLY2, a conformation with the amino acid backbone characterized by an intramolecular OH···N H-bond. These complexes are clearly predicted to be less stable, since this intramolecular H-bond is broken after intermolecular H-bond complexation. Furthermore, complexes **5** and **6** have other type of intermolecular H-bonds. In these complexes, the OH of the amino acid is still the H-bond donor but the N atom of the $NH_2$ group is the acceptor site. The donor and acceptor sites of 1MU do not differ from the other complexes and, once again, the $C^4{=}O$ H-bond acceptor site is energetically favored compared to the $C^2{=}O$ acceptor site.

The calculated H-bond interaction energies of the obtained complexes are listed in Table 4. Since the three different conformations of glycine are clearly present in the configurations of the complexes, these conformations were taken into

**Table 4. Relative H-Bond Interaction Energies, BSSE-Corrected H-Bond Interaction Energies, and ZPE- and BSSE-Corrected H-Bond Interaction Energies (kJ·mol$^{-1}$) for the H-Bonded Complexes Glycine·1-Methyluracil at the DFT(B3LYP)/6-31++G** and MP2(6-31++G**) Levels of Theory**

| | H-bond interaction energies | | |
|---|---|---|---|
| | $\Delta E$ | $\Delta E$ (BSSE corrected) | $\Delta E$ (ZPE and BSSE corrected) |
| | | DFT | |
| complex **1** | −59.29 | −55.95 | −54.14 |
| complex **2** | −54.46 | −51.54 | −49.60 |
| complex **3** | −61.16 | −57.88 | −56.58 |
| complex **4** | −55.77 | −52.90 | −51.37 |
| complex **5** | −34.49 | −28.94 | −26.83 |
| complex **6** | −30.92 | −25.89 | −23.85 |
| | | MP2 | |
| complex **1** | −63.60 | −49.64 | −47.83 |
| complex **2** | −60.83 | −47.11 | −45.17 |
| complex **3** | −61.59 | −47.53 | −46.23 |
| complex **4** | −60.83 | −44.75 | −43.21 |
| complex **5** | −49.78 | −30.56 | −28.45 |
| complex **6** | −47.59 | −28.43 | −26.39 |


dx.doi.org/10.1021/jp307388e | J. Phys. Chem. B 2012, 116, 11890−11898

account to obtain the H-bond interaction energies. The (basis set superposition error) BSSE and the ZPE corrections were also taken into account. From Table 4, it is clear that the $C^4$═O site in 1MU is a better H-bond acceptor than the $C^2$═O site since the H-bond interaction energies for the complexes **2**, **4**, and **6**, all with the $C^2$═O as acceptor, are smaller than for the similar complexes **1**, **3**, and **5** with the $C^4$═O as acceptor site. The interaction energy is much smaller for complexes **5** and **6** since the strong intramolecular H-bond in the monomer glycine conformation is broken to allow complex formation with 1MU.

As complex **1** is by 4.55 kJ·mol$^{-1}$ the most stable H-bonded complex as well as it is formed of conformation GLY1 which is the most abundant conformation of the monomer, it is reasonable to limit the search for H-bond complexes, which are only present in a small concentration in the matrix, to complex **1** only.

The theoretical (DFT) FT-IR spectrum of the most stable glycine·1-methyluracil complex as well as the spectra of the monomers, i.e., the keto tautomer of 1MU and the conformation GLY1, are presented in Figure 5. Compared to the monomers, the H-bond sensitive modes such as $\nu$(OH), $\nu$(NH), and $\nu$(C═O) are shifted in the complex. Furthermore, there are six new intramolecular modes. These shifts and new modes can be used to observe the complex in the matrix-isolation FT-IR spectrum.

In the matrix-isolation experiment, the two complex partners were sublimated from a dual furnace, each at its optimal sublimation temperature, i.e., 343 K for glycine and 313 K for 1MU. The overall FT-IR spectrum of the complex is shown in Figure 6 together with the spectra of the monomers. The

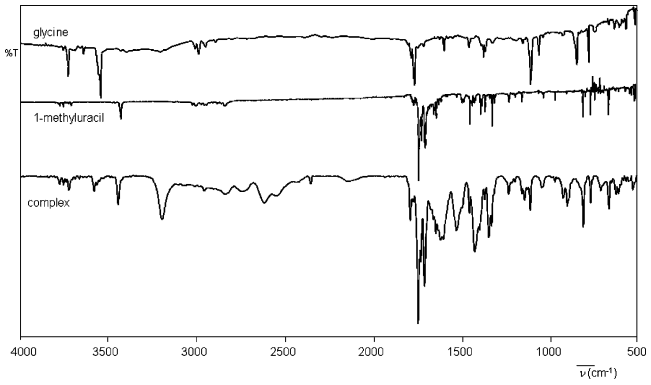


**Figure 6.** Experimental transmission (% T) FT-IR spectra of glycine, 1-methyluracil, and the complex glycine·1-methyluracil in Ar at 16 K.

complex spectrum is almost free of contaminants, especially water, as can be seen in the region 3800−3700 cm$^{-1}$. This is important when H-bonded complexes are analyzed (Figure 6). Furthermore, this is an indication that the newly developed dual furnace is working well and that no decomposition of the compounds occurs. The FT-IR spectrum of the complex will be separately discussed for three different regions, i.e., 3600−2350, 1900−1000, and 1050−500 cm$^{-1}$.

**3600−2350 cm$^{-1}$.** The high-frequency region of the FT-IR is presented in Figure 7. In this region the $\nu$(XH) modes are located. Since the $\nu$(OH) and the $\nu$(NH) are involved in intramolecular H-bonds, their intensities are increased and their frequencies are red-shifted.

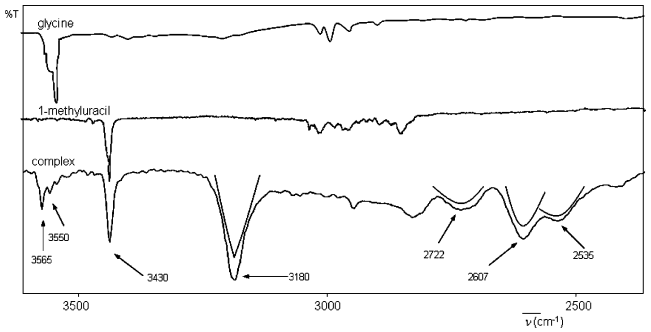


**Figure 7.** High-frequency region (3600−2350 cm$^{-1}$) of the transmission (% T) FT-IR spectra of glycine, 1-methyluracil, and the glycine·1-methyluracil complex in Ar at 16 K.

In the monomer spectrum the $\nu$(OH) mode is observed at 3564/3548 cm$^{-1}$ for GLY1 and at 3559 cm$^{-1}$ for GLY2. The $\nu$(OH···) mode involved in a OH···N H-bond of the low-abundance conformation GLY3 is weakly observed at 3200 cm$^{-1}$. In the spectrum of the complex, the monomer $\nu$(OH) bands of GLY1 and GLY2 are observed at 3565 and 3550 cm$^{-1}$, respectively. The $\nu$(OH···) mode of the complex involved in an intermolecular H-bond is predicted as a very intense band at 2952 cm$^{-1}$ (Table 5). In the spectrum there are three new, broad bands observed with maxima at 2722, 2607, and 2535 cm$^{-1}$. Since the $\nu$(OH···) modes of the less stable complexes **2** and **3** are very intensely predicted at 3057 and 2929 cm$^{-1}$, the band at 2722 cm$^{-1}$ can be assigned to complex **2**, the most intense band at 2607 cm$^{-1}$ to the most stable configuration, i.e., complex **1**, and the band at 2535 cm$^{-1}$ to complex **3**. It is not uncommon to observe experimental bands at considerably smaller wavenumbers than predicted due to the enhanced anharmonicity caused by the H-bond, which is not fully taken into account by the scaling factors used.[49,50]

The $\nu$(NH) mode of the 1MU monomer is observed at 3428 cm$^{-1}$ in the monomer spectrum and at the nearly similar frequency of 3430 cm$^{-1}$ in the spectrum of the complex. The H-bond-involved $\nu$(NH···) mode of complex **1** is predicted at 3106 cm$^{-1}$. In the spectrum of the complex, a new broader band appears at 3180 cm$^{-1}$. Since this is the only intense broad band in the region 3300−3000 cm$^{-1}$, this band must be assigned to this bonded $\nu$(NH···) mode. This H-bond-involved mode is predicted to be more intense than $\nu$(OH···) ($\sum I(\nu(\mathrm{NH}))$ = 5141 km·mol$^{-1}$ compared to $\sum I(\nu(\mathrm{OH}))$ = 3600 km·mol$^{-1}$), and considering the relative experimental intensities at 3180 cm$^{-1}$ and at 2722 + 2607 + 2535 cm$^{-1}$, this band must be a superposition of the $\nu$(NH···) modes of all the complexes present. This is in accordance with the predicted theoretical values of 3143 cm$^{-1}$ for complex **2** and 3091 cm$^{-1}$ for complex **3**.

An extra argument to demonstrate the intermolecular H-bond complexation in the FT-IR spectrum is the ratio of the intensities of the $\nu$(NH) mode of monomeric 1MU at 3430 cm$^{-1}$ and the $\delta(C^5H)$ mode at 1222 cm$^{-1}$, one of the clearly nonoverlapping bands, which is not influenced by the complexation. In the spectrum of monomeric 1MU, the ratio of $I(\nu(\mathrm{NH}))/I(\delta(C^5H))$ is 2.0, which is reduced to 1.6 in the spectrum of the complex. This decrease demonstrates that part of the 1MU molecules do not occur as monomer but rather are involved in H-bonded complexes, of which the $\nu$(NH) mode is observed in a shifted vibrational mode.


dx.doi.org/10.1021/jp307388e | J. Phys. Chem. B 2012, 116, 11890−11898

Table 5. Experimentally Observed Frequencies ($cm^{-1}$), Frequency Shifts ($cm^{-1}$), and Theoretical (DFT(B3LYP)/6-31++G**) Frequencies ($cm^{-1}$) and Intensities ($km \cdot mol^{-1}$) of the Most Important Modes of the Complex Glycine·1-Methyluracil Compared to Experimentally Observed Frequencies of the Monomers ($cm^{-1}$)

| complex | | | | glycine | 1-methyluracil | |
|---|---|---|---|---|---|---|
| $\bar{\nu}^a$ | $\bar{\nu}^b$ | $I$ | shift[c] | $\bar{\nu}^a$ | $\bar{\nu}^a$ | $\bar{\nu}^b$ |
| 3180 | 3106 | 1649 | −248 | | 3428 | $\nu$(NH···) (complex **1**) |
| | 3143 | 1749 | −248 | | 3428 | $\nu$(NH···) (complex **2**) |
| | 3091 | 1743 | −248 | | 3428 | $\nu$(NH···) (complex **3**) |
| 2722 | 3057 | 695 | −834[c] | 3564−3548 | | $\nu$(OH···) (complex **2**) |
| 2607 | 2952 | 1432 | −949[c] | 3564−3548 | | $\nu$(OH···) (complex **1**) |
| 2535 | 2929 | 1473 | −1024 | 3559 | | $\nu$(OH···) (complex **3**) |
| 1722 | 1712 | 1018 | −59 | 1781 | | $\nu$(C═O···) |
| 1610 | 1675 | 474 | −90 | | 1700 | $\nu$($C_4$═O) |
| 1520 | 1490 | 55 | +132 | | 1388 | $\delta$(NH···) |
| 1486 | 1458 | 25 | +101 | | 1385 | $\delta$(NH···) |
| 1415 | 1431 | 11 | +282 | 1133 | | $\delta$(OH) |
| 1338 | 1338 | 5 | +205 | 1133 | | $\delta$(OH) |
| 1034 | 976 | 83 | +416 | 618 | | $\gamma$(OH) |
| 917 | 895 | 42 | +258 | | 659 | $\gamma$(NH) |

[a]Observed frequency in the matrix-isolation FT-IR spectrum. [b]Theoretical predicted frequency of the complex using variable scaling factors for DFT: 0.95 for (X−H); 0.98 for $\gamma$ and $\tau$; 0.975 for all other modes. [c]Experimental frequency shift is calculated in relation to the mean frequency, i.e., $(\nu^1 + \nu^2)/2$. [d]Only the most important potential energy contribution is listed.

**1900−1000 $cm^{-1}$.** The spectral region 1900−1000 $cm^{-1}$ is shown in Figure 8. This region contains the H-bond-involved modes $\nu$(C═O), $\delta$(OH), and $\delta$(NH).

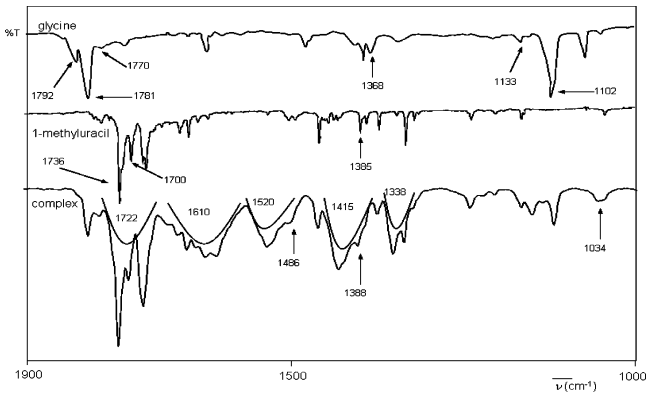


**Figure 8.** Frequency region 1900−1000 $cm^{-1}$ of the transmission (% T) FT-IR spectra of glycine, 1-methyluracil, and the glycine·1-methyluracil complex in Ar at 16 K.

The $\nu$(C═O) absorption is predicted as a very intense band. This mode occurs at 1736 and 1700 $cm^{-1}$ for the $C^2$═O and $C^4$═O groups of 1MU in the monomer spectrum, whereas in the monomer spectrum of glycine this mode is observed at 1781 $cm^{-1}$ (GLY1), 1792 $cm^{-1}$ (GLY2), and 1770 $cm^{-1}$ (GLY3), respectively. In the spectrum of the complex, the monomer bands of glycine occur at 1782 $cm^{-1}$ (GLY1) with shoulders at 1692 $cm^{-1}$ (GLY2) and 1765 $cm^{-1}$ (GLY3). The non-H-bonded modes of 1MU are observed at 1736 and 1700 $cm^{-1}$. The shifted modes due to the H-bonded species are predicted at 1712 $cm^{-1}$ for $\nu$(C═O···) of glycine and 1675 $cm^{-1}$ for $\nu$(C═O···) of 1MU. The first one is observed in the increased broadening around 1722 $cm^{-1}$. The second one occurs as a broad band with a maximum around 1610 $cm^{-1}$.

The 1MU $\delta$(NH···) mode in the complexes has significant potential energy contributions to the modes predicted at 1490 and 1458 $cm^{-1}$. These absorptions are observed in the broad bands at 1520 and 1486 $cm^{-1}$. This mode is clearly shifted since $\delta$(NH) bands of monomeric 1MU are observed in the monomer spectrum at 1385 $cm^{-1}$ and at 1388 $cm^{-1}$.

Since the OH group of the amino acid glycine is involved in the H-bonds, the glycine $\delta$(OH) mode is also shifted. The $\delta$(OH) mode of the non-H-bonded conformations GLY1 and GLY2 is observed at 1133 and 1102 $cm^{-1}$, respectively. The intramolecular H-bond involved mode $\delta$(OH···) of GLY3 is observed at 1368 $cm^{-1}$. In the complexes, this mode has potential energy contributions to the bands predicted at 1431 and 1338 $cm^{-1}$. The first band is experimentally observed as a broad band at 1415 $cm^{-1}$ while the latter is observed as a broad band at 1338 $cm^{-1}$.

**1050−500 $cm^{-1}$.** The low-frequency region of the FT-IR spectrum of the complex glycine·1MU is presented in Figure 9.

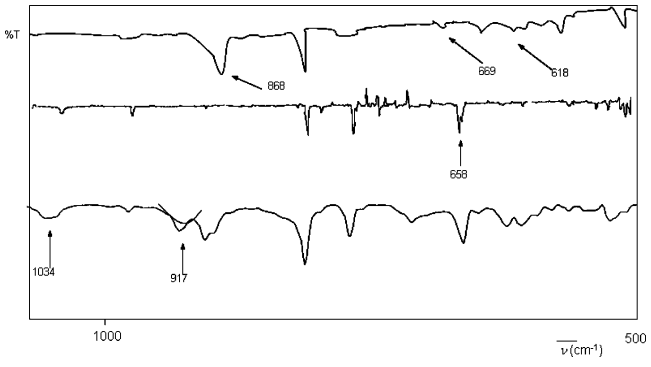


**Figure 9.** Low-frequency region (1050−500 $cm^{-1}$) of the transmission (% T) FT-IR spectra of glycine, 1-methyluracil, and the glycine·1-methyluracil complex in Ar at 16 K.

This region contains the out-of-plane modes of the NH and OH groups which are involved in the H-bonding. The $\gamma$(OH) mode is observed at 618 $cm^{-1}$ (GLY1), 868 $cm^{-1}$ (GLY2), and 669 $cm^{-1}$ (GLY3) in the spectrum of monomer glycine. In the complex, this mode is theoretically predicted to be strongly blue-shifted toward 976 $cm^{-1}$. Since the complex $\gamma$(OH···)


dx.doi.org/10.1021/jp307388e | J. Phys. Chem. B 2012, 116, 11890−11898

mode is expected to be broad, the absorption observed at 1034 $cm^{-1}$ can be assigned to $\gamma$(OH···).

The $\gamma$(NH) mode of 1MU is observed at 659 $cm^{-1}$ in the monomer spectrum. After complexation, this mode is predicted at 895 $cm^{-1}$ and in the experimental spectrum it is observed at 917 $cm^{-1}$. Another evidence for the presence of the complex is obtained from the ratio of the intensities of $\gamma$(NH) of 1MU and $\delta(C^5H)$ at 1222 $cm^{-1}$, assigned to the mode not influenced by the H-bonding. In the monomer spectrum of 1MU the ratio $I(\gamma(NH))/I(\delta(C^5H))$ is 2.8, which decreases to 1.7 in the spectrum of the complex. This demonstrates that the $\gamma$(NH) mode is shifted due to complexation; as a matter of fact, a part of the 1MU molecules do not occur as monomers but are involved in H-bonded complexes.

For the glycine·1MU complex, the six new intermolecular modes are all predicted between 275 and 33 $cm^{-1}$ (Table 6), i.e., below the region studied here (<400 $cm^{-1}$).

**Table 6. Theoretical DFT(B3LYP)/6-31++G** Frequencies ($cm^{-1}$) and Intensities of the New Intermolecular Modes of the H-Bonded Complex Glycine·1-Methyluracil**

| $\bar{\nu}^a$ | $I$ | mode |
|---|---|---|
| 275 | 44 | $\nu$ |
| 143 | 8 | $\nu$ |
| 116 | 2 | $\delta$ |
| 65 | 2 | $\delta$ |
| 44 | <1 | $\tau$ |
| 33 | 5 | $\gamma$ |

[a]Variable scaling factors for DFT: 0.95 for (X−H); 0.98 for $\gamma$ and $\tau$; 0.975 for all other modes.

## DISCUSSION

The most stable configurations for the complexes GLY·1MU appear to be those with the carbonyl and hydroxyl group of the amino acid interacting with the proton donor and acceptor groups of the nucleic acid base. These structures have two strong H-bonds. The stabilization energies for the most stable complex obtained in this work are −54.14 (MP2) or −47.83 kJ·$mol^{-1}$ (DFT) for GLY·MU. This implies a stabilization of −25 to −30 kJ·$mol^{-1}$ per H-bond. These are typical values for closed H-bond systems as demonstrated by literature values for different closed H-bonded systems (Table 7).

**Table 7. DFT H-Bond Interactions Energies (kJ·$mol^{-1}$) of Closed H-Bonded Systems**

| complex | H-bond interaction energy |
|---|---|
| formic acid dimer[57] | −63.0 |
| formamide dimer[58] | −59.6 |
| glycine·uracil[24] | −64.6 |
| leucine·adenine[18] | −55 |
| glycine·1MU | −47.83 |

The strength of a H-bond is to a large extent determined by the distance between the proton (XH) and the acceptor (Y) groups. H-bonding is accompanied by a considerable increase of the XH distance and a red shift of the H-bond-involved stretching mode $\nu$(XH···) as well as a blue shift for the bending $\delta$(XH···) and out-of-plane modes $\gamma$(XH···). These H-bond properties of the complexes studied in this work are compared to reported data of comparable H-bonded complexes in the literature (Table 8).

When a H-bond becomes stronger, the H-bond-sensitive modes such as $\nu$(XH···), $\delta$(XH···), and $\gamma$(XH···) are more shifted. The relation between the value of the red shift of the stretching vibration $\nu$(XH) and the blue shift of the out-ofplane vibration $\gamma$(XH) is presented in Figure 10. The data in this figure are limited to $\Delta\gamma$ shifts smaller than 450 $cm^{-1}$. From this figure, a general linear relationship is observed between $-\Delta\nu$ and $\Delta\gamma$, independent of the type of H-bond.

The formation of the H-bond is also accompanied by an increase of the XH distance compared to the XH distance in the non-H-bonded compound. This distance increase arises from the weakening of the X−H bond due to charge transfer from the acceptor lone pair to the antibonding $\sigma_u$* molecular orbital of X−H. The relation of the relative distance increase $\Delta r(XH)/r^\circ$ and the relative frequency shift $\Delta\nu(XH)/\nu^\circ$ is shown in Figure 11. Both parameters appears to be in linear relationship. In contrast to the distance $r$(XH), the relative distance increase $\Delta r(XH)/r^\circ$ is independent of the type of H-bond. This implies that the parameter $\Delta r(XH)/r^\circ$ can be used to quantify the strength of the H-bond, independently of the type of H-bond.

## CONCLUSIONS

The H-bond interaction between glycine and 1-methyluracil was theoretically investigated starting from the most stable monomeric compounds at the DFT(B3LYP)/6-31G level of theory. The accuracy of the geometries obtained at this level was evaluated with single-point energy calculations on the structures optimized at this and at the DFT(B3LYP)/6-31++G** level. This evaluation revealed that the DFT(B3LYP)/6-31G optimized geometries yield satisfying structures.

The most stable complex is formed with the most stable glycine conformation which results in a closed H-bonded complex with 1MU. The carboxylic acid group serves as both a H-bond donor (OH) and a H-bond acceptor (C═O) in the amino acid. The NH group is the H-donor site in 1MU and the $C^4$═O appears to be the better acceptor site. The obtained H-bond stabilization energy for the most stable complex is −47.83 kJ·$mol^{-1}$ at the MP2 level and −54.14 kJ·$mol^{-1}$ with the DFT(B3LYP) method.

A newly developed dual furnace was used to sublimate both glycine and 1MU, each at its optimal sublimation temperature, and the matrix-isolation FT-IR spectrum was registered. The 3-fold absorption due to the $\nu$(OH···) modes of glycine suggests the presence of three different glycine·1MU complexes in the matrix. The observation of the other H-bond-involved modes $\nu$(NH···), $\nu$(C═O···), $\delta$(NH···), $\delta$(OH···), $\gamma$(NH···), and $\gamma$(OH···) demonstrates clearly the presence of the complex in the matrix. Furthermore, the intensities of the $\nu$(NH) and $\gamma$(NH) are decreased compared to the non-H-bonded mode $\delta(C^5H)$ of 1MU, which demonstrates that these modes were shifted due to the H-bonding in the complex.

The new intermolecular modes which arise due to the complexation could not be observed in the matrix since these are located below the studied region.

The properties of the H-bonds were evaluated. The correlations between the relative distance increase $\Delta r(XH)/r^\circ$ and the relative frequency shift $\Delta\nu(XH)/\nu^\circ$ and the frequency shifts $-\Delta\nu$ and $\Delta\gamma$ appeared to be linear and independent of the type of H-bond.


dx.doi.org/10.1021/jp307388e | J. Phys. Chem. B 2012, 116, 11890−11898

**Table 8. H-Bond Properties of Closed H-Bonded Complexes**

| structure | H-bond type | H-bond interaction energy (kJ·mol$^{-1}$) | $r$(Y···H) (Å) | $r$(XH) (Å) | $\Delta r$(XH)[a] | (Y···HX) angle (deg) | $\Delta\nu$ (XH)[a] (cm$^{-1}$) | $\Delta\gamma$ (XH)[a] (cm$^{-1}$) |
|---|---|---|---|---|---|---|---|---|
| GLY·1MU | | | | | | | | |
| complex **1** | C═O$^{1MU}$···HO$^{GLY}$ | −55.95 | 1.653 | 1.004 | 0.031 | 176 | −610 | +387 |
| | NH$^{1MU}$···O═C$^{GLY}$ | | 1.839 | 1.033 | 0.019 | 167 | −323 | +242 |
| complex **2** | C═O$^{1MU}$···HO$^{GLY}$ | −51.54 | 1.674 | 1.000 | 0.027 | 177 | −505 | +306 |
| | NH$^{1MU}$···O═C$^{GLY}$ | | 1.866 | 1.032 | 0.018 | 167 | −286 | +228 |
| complex **3** | C═O$^{1MU}$···HO$^{GLY}$ | −57.88 | 1.643 | 1.006 | 0.033 | 176 | −635 | +337 |
| | NH$^{1MU}$···O═C$^{GLY}$ | | 1.831 | 1.034 | 0.020 | 167 | −338 | +248 |
| complex **4** | C═O$^{1MU}$···HO$^{GLY}$ | −52.90 | 1.687 | 0.999 | 0.026 | 177 | −534 | +301 |
| | NH$^{1MU}$···O═C$^{GLY}$ | | 1.871 | 1.032 | 0.018 | 167 | −298 | +232 |
| complex **5**[a] | C═O$^{1MU}$···HO$^{GLY}$ | −28.94 | 1.707 | 0.993 | 0.020 | 171 | −408 | +233 |
| | NH$^{1MU}$···N$^{GLY}$ | | 1.849 | 1.047 | 0.033 | 172 | −587 | +364 |
| complex **6**[a] | C═O$^{1MU}$···HO$^{GLY}$ | −25.89 | 1.717 | 0.991 | 0.018 | 169 | −343 | +210 |
| | NH$^{1MU}$···N$^{GLY}$ | | 1.850 | 1.047 | 0.033 | 172 | −553 | +359 |
| glycine.uracil[24] | O$^{U}$···HO$^{GLY}$ | −62.6 | 1.663 | 1.003 | 0.030 | 177 | 599 | |
| | NH$^{U}$···O═C$^{GLY}$ | | 1.783 | 1.033 | | 171 | 378 | |

[a]The values $\Delta r$, $\Delta\nu$, and $\Delta\gamma$ for these complexes were calculated relative to the mean value of GLY1 and GLY3 since the monomer GLY2 contains an intramolecular OH···N H-bond.

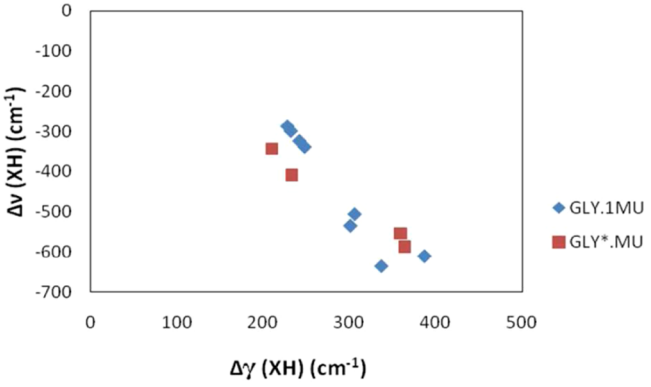


**Figure 10.** Correlation between the stretching $\nu$(XH) and the out-of-plane $\gamma$(XH) frequency shift in different closed H-bonded complexes of glycine·1MU (GLY·1MU for complexes **1**−**4** and GLY*·1MU for complexes **5** and **6**).

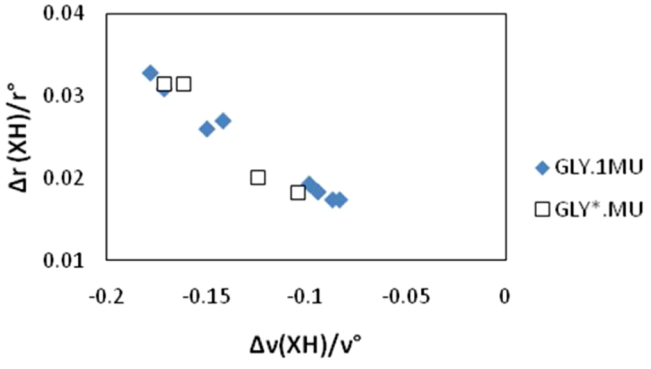


**Figure 11.** Correlation between the relative X−H distance increase $\Delta r$(XH)/$r°$ and the relative stretching frequency shift $\Delta\nu$(XH)/$\nu°$ in closed H-bonded complexes of glycine·1MU (GLY·1MU for complexes **1**−**4** and GLY*·1MU for complexes **5** and **6**).

## ■ ASSOCIATED CONTENT

### Supporting Information

Important theoretical and observed FT-IR frequencies of glycine and 1-methyluracil in the argon matrix and extended energy data; extended results of frequency analysis on the DFT(B3LYP)/6-31++G** level of theory. This material is available free of charge via the Internet at http://pubs.acs.org.

## ■ AUTHOR INFORMATION

### Corresponding Author

*E-mail: boeckx@hotmail.com.

### Notes

The authors declare no competing financial interest.

## ■ ACKNOWLEDGMENTS

This research was funded by the Department of Chemistry of the University of Leuven and was conducted utilizing the high-performance computational resources provided by the University of Leuven, http://ludit.kuleuven.be/hpc.

## ■ REFERENCES

(1) Stivers, J. T.; Jiang, Y. L. *Chem. Rev.* **2003**, *103*, 2729−2759.
(2) Beamer, L. J.; Pabo, C. O. *J. Mol. Biol.* **1992**, *227*, 177−196.
(3) Iftode, C.; Daniely, Y.; Borowiec, J. A. *Crit. Rev. Biochem. Mol.* **1999**, *34*, 141−180.
(4) Spiegelman, B. M.; Heinrich, R. *Cell* **2004**, *119*, 157−167.
(5) Sandman, K.; Pereira, S. L.; Reeve, J. N. *Cell. Mol. Life Sci.* **1998**, *54*, 1350−1364.
(6) Thomas, J. *J. Biochem. Soc. Trans.* **2001**, 395−401.
(7) Tang, K.; Sun, H. T.; Zhou, Z. Y.; Wang, Z. Z. *Int. J. Quantum Chem.* **2008**, *108*, 1287−1293.
(8) Li, Y. M.; Zhou, X. M.; Tang, K.; Qin, M.; Zhou, Z. Y. *Indian J. Chem., Sect. A* **2010**, *49*, 145−150.
(9) Brejc, K.; Sixma, T. K.; Kitts, P. A.; Kain, S. R.; Tsien, R. Y.; Ormo, M.; Remington, S. *Proc. Natl. Acad. Sci. U.S.A.* **1997**, *94*, 2306−2311.
(10) Fromme, J. C.; Bruner, S. D.; Yang, W.; Karplus, M.; Verdine, G. L. *Nat. Struct. Biol.* **2003**, *10*, 204−211.
(11) Norman, D. P. G.; Chung, S. J.; Verdine, G. L. *Biochemistry* **2003**, *42*, 1564−1572.
(12) Chitester, B. J.; Walz, F. G. *Arch. Biochem. Biophys.* **2002**, *406*, 73−77.
(13) Walz, F. G.; Osterman, H. L.; Libertin, C. *Arch. Biochem. Biophys.* **1979**, *195*, 95−102.
(14) Cheng, A. C.; Frankel, A. D. *J. Am. Chem. Soc.* **2004**, *126*, 434−435.

(15) Wetmore, S. D.; Boyd, R. J.; Eriksson, L. A. *Chem. Phys. Lett.* **2000**, *322*, 129−135.
(16) Wesolowski, S. S.; Leininger, M. L.; Pentchev, P. N.; Schaefer, H. F. *J. Am. Chem. Soc.* **2001**, *123*, 4023−4028.
(17) Jalbout, A. F.; Adamowicz, L. *J. Phys. Chem. A* **2001**, *105*, 1071−1073.
(18) Zhao, Y.; Zhou, L. X. *Theor. Chem. Acc.* **2005**, *113*, 249−256.
(19) Sander, W.; Roy, S.; Polyak, I.; Ramirez-Anguita, J. M.; Sanchez-Garcia, E. *J. Am. Chem. Soc.* **2012**, *134*, 8222−8230.
(20) Pettersson, M. Investigations of I2-Xe and I2-benzene complexes in solid Krypton by coherent and spontanuous Raman spectroscopy. In the 8th International Conference on Low Temperature Chemistry, Yerevan, Armenia; 2010.
(21) Sarai, A.; Saito, M. *Int. J. Quantum Chem.* **1984**, *25*, 527−533.
(22) Sarai, A.; Saito, M. *Int. J. Quantum Chem.* **1985**, *28*, 399−409.
(23) Otto, P.; Clementi, E.; Ladik, J.; Martino, F. *J. Chem. Phys.* **1984**, *80*, 5294−5302.
(24) Pichierri, F.; Aida, M.; Gromiha, M. M.; Sarai, A. *J. Am. Chem. Soc.* **1999**, *121*, 6152−6157.
(25) Dabkowska, I.; Rak, J.; Gutowski, M. *J. Phys. Chem. A* **2002**, *106*, 7423−7433.
(26) Dabkowska, I.; Gutowski, M.; Rak, J. *Pol. J. Chem.* **2002**, *76*, 1243−1247.
(27) Dabkowska, I.; Gutowski, M.; Rak, J. *J. Am. Chem. Soc.* **2005**, *127*, 2238−2248.
(28) He, Q.; Huo, A. X.; Meng, X. J.; Yang, J. *Chin. J. Chem.* **2010**, *29*, 738−746.
(29) Peral, F.; Troitino, D. *J. Mol. Struct. (THEOCHEM)* **2010**, *944*, 1−11.
(30) Adamiak, D. A.; Milecki, J.; Adamiak, R. W.; Rypniewski, W. *New J. Chem.* **2010**, *34*, 903−909.
(31) Bende, A. *Theor. Chem. Acc.* **2010**, *125*, 253−268.
(32) Mishra, D.; Pal, S. *J. Mol. Struct. (THEOCHEM)* **2009**, *902*, 96−102.
(33) Liu, A. Z.; Wang, J. F.; Lu, Z. W.; Yao, L. S.; Li, Y.; Yan, H. G. *ChemBioChem.* **2008**, *9*, 2860−2871.
(34) Galetich, I.; Kosevich, M.; Shelkovsky, V.; Stepanian, S. G.; Blagoi, Y. P.; Adamowicz, L. *J. Mol. Struct.* **1999**, *478*, 155−162.
(35) Smolyaninova, T.; Bruskov, V.; Kashparova, Y. *Mol. Biol. (Russian)* **1985**, *19*, 992.
(36) Helene, C.; Lancelot, G. *Prog. Biophys. Mol. Biol.* **1982**, *39*, 1−68.
(37) Galetich, I.; Stepanian, S. G.; Shelkovsky, V.; Kosevich, M.; Blagoi, Y. P.; Adamowicz, L. *J. Phys. Chem. B* **1999**, *103*, 11211−11217.
(38) Gutowski, M.; Dabkowska, I.; Rak, J.; Xu, S.; Nilles, J. M.; Radisic, D.; Bowen, K. H. *Eur. Phys. J. D* **2002**, *20*, 431−439.
(39) Dabkowska, I.; Rak, J.; Gutowski, M.; Nilles, J. M.; Stokes, S. T.; Radisic, D.; Bowen, K. H. *Phys. Chem. Chem. Phys.* **2004**, *6*, 4351−4357.
(40) Storoniak, P.; Mazurkiewicz, K.; Haranczyk, M.; Gutowski, M.; Rak, J.; Eustis, S. N.; Ko, Y. J.; Wang, H. P.; Bowen, K. H. *J. Phys. Chem. B* **2010**, *114*, 11353−11362.
(41) Ramaekers, R.; Pajak, J.; Lambie, B.; Maes, G. *J. Chem. Phys.* **2004**, *120*, 4182−4193.
(42) Ramaekers, R.; Pajak, J.; Maes, G. *Asian Chem. Lett.* **2004**, *2 & 3*, 203−209.
(43) Smets, J.; Adamowicz, L.; Maes, G. *J. Phys. Chem.* **1996**, *100*, 6434−6444.
(44) Graindourze, M.; Smets, J.; Zeegers-Huyskens, T.; Maes, G. *J. Mol. Struct.* **1990**, *222*, 345−364.
(45) Becke, A. D. *Phys. Rev. A* **1988**, *38*, 3098−3100.
(46) Lee, C. T.; Yang, W. T.; Parr, R. G. *Phys. Rev. B* **1988**, *37*, 785−789.
(47) Moller, C.; Plesset, M. S. *Phys. Rev.* **1934**, *46*, 618−622.
(48) Boeckx, B.; Maes, G. *J. Phys. Chem. A* **2012**, *116*, 1956−1965.
(49) Boeckx, B.; Ramaekers, R.; Maes, G. *J. Biophys. Chem.* **2011**, *159*, 247−256.
(50) Boeckx, B.; Maes, G. *Spectrochim. Acta, Part A* **2012**, *86*, 366−374.
(51) Frisch, M. J.; Trucks, G. W.; Schlegel, H. B.; Scuseria, G. E.; Robb, M. A.; Cheeseman, J. R.; Montgomery, J. A.; Vreven, T.; Kudin, K. N.; Burant, J. C.; et al. *Gaussian 03, Revision B.05*; Gaussian Inc.: Wallingford, CT, 2003.
(52) Rostkowska, H.; Lapinski, L.; Nowak, M. J. *Vib. Spectrosc.* **2009**, *49*, 43−51.
(53) Boeckx, B.; Ramaekers, R.; Maes, G. *J. Mol. Spectrosc.* **2010**, *261*, 73−81.
(54) Boeckx, B.; Nelissen, W.; Maes, G. *J. Phys. Chem. A* **2012**, *116*, 3247−3258.
(55) Muzomwe, M.; Boeckx, B.; Maes, G.; Kasende, O. E. S. *Afr. J. Chem.* **2011**, *64*, 23−33.
(56) Boeckx, B.; Maes, G. *J. Biophys. Chem.* **2012**, *165−166*, 62−73.
(57) Schuerman, G. S.; Van Meervelt, L.; Loakes, D.; Brown, D. W.; Lin, P. K. T.; Moore, M. H.; Salisbury, S. A. *J. Mol. Biol.* **1998**, *282*, 1005−1011.
(58) Stepanian, S. G.; Reva, I. D.; Radchenko, E. D.; Rosado, M. T. S.; Duarte, M. L. T. S.; Fausto, R.; Adamowicz, L. *J. Phys. Chem. A* **1998**, *102*, 1041−1054.
(59) Pecul, M.; Leszczynski, J.; Sadlej, J. *J. Chem. Phys.* **2000**, *112*, 7930−7938.
(60) Vargas, R.; Garza, J.; Friesner, R. A.; Stern, H.; Hay, B. P.; Dixon, D. A. *J. Phys. Chem. A* **2001**, *105*, 4963−4968.